JACS
JOURNAL OF THE AMERICAN CHEMICAL SOCIETY
Article
pubs.acs.org/JACS

Repair of Hydantoin Lesions and Their Amine Adducts in DNA by Base and Nucleotide Excision Repair

Paige L. McKibbin,[†] Aaron M. Fleming,[‡] Mohammad Atif Towheed,[§] Bennett Van Houten,[§] Cynthia J. Burrows,[‡] and Sheila S. David*[,†]

[†]Department of Chemistry, University of California, Davis, One Shields Avenue, Davis, California 95616, United States
[‡]Department of Chemistry, University of Utah, 315 South 1400 East, Salt Lake City, Utah 84112, United States
[§]Department of Pharmacology and Chemical Biology, University of Pittsburgh Cancer Institute, University of Pittsburgh, 5117 Centre Avenue, Pittsburgh, Pennsylvania 15213, United States

Supporting Information

ABSTRACT: An important feature of the common DNA oxidation product 8-oxo-7,8-dihydroguanine (OG) is its susceptibility to further oxidation that produces guanidinohydantoin (Gh) and spiroiminodihydantoin (Sp) lesions. In the presence of amines, G or OG oxidation produces hydantoin amine adducts. Such adducts may form in cells via interception of oxidized intermediates by protein-derived nucleophiles or naturally occurring amines that are tightly associated with DNA. Gh and Sp are known to be substrates for base excision repair (BER) glycosylases; however, large Sp−amine adducts would be expected to be more readily repaired by nucleotide excision repair (NER). A series of Sp adducts differing in the size of the attached amine were synthesized to evaluate the relative processing by NER and BER. The UvrABC complex excised Gh, Sp, and the Sp−amine adducts from duplex DNA, with the greatest efficiency for the largest Sp−amine adducts. The affinity of UvrA for all of the lesion duplexes was found to be similar, whereas the efficiency of UvrB loading tracked with the efficiency of UvrABC excision. In contrast, the human BER glycosylase NEIL1 exhibited robust activity for all Sp−amine adducts irrespective of size. These studies suggest that both NER and BER pathways mediate repair of a diverse set of hydantoin lesions in cells.

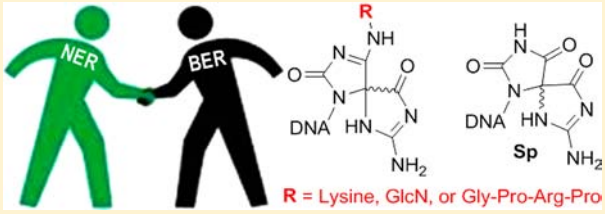

INTRODUCTION

Cellular respiration and the inflammatory response generate reactive oxygen and nitrogen species (RONS), resulting in DNA modifications that contribute to premature aging, mutagenesis, and carcinogenesis.[1−3] Of the various oxidized bases that may be formed, 8-oxo-7,8-dihydroguanine (OG) has been the most extensively studied[1,2,4] and shown to be highly mutagenic in the absence of repair.[1] A distinct feature of OG is its susceptibility to further oxidation that leads to formation of the hydantoin lesions, guanidinohydantoin (Gh) and the two diastereomers of spiroiminodihydantoin (Sp1 and Sp2) (Figure 1).[4−8] Gh and Sp have been established as the major products of G and OG oxidation by peroxynitrite, peroxyl radicals, and hypochlorous acid, reactive species that are present in cells during an inflammatory response.[9−20] Recently, Gh and Sp lesions were detected in the liver and colon tissue of *Rag2*$^{-/-}$ mice at levels 100-fold lower than that of OG.[3] Oxidative conditions are also known to mediate formation of DNA−protein cross-links (DPC), DNA−DNA cross-links, and DNA−polyamine adducts.[21−25] *In vitro*, covalent cross-links between DNA and proteins have been shown to form under oxidative conditions when the DNA contains the OG lesion.[21,24] Indeed, oxidation with a number of biologically relevant oxidants in the presence of DNA binding proteins has been shown to produce hydantoin−protein cross-links.[26] These previous studies suggest that in a cellular environment a wide variety of hydantoin lesion structures may be present.

Polymerase primer extension and cellular mutation assays using synthetic DNA oligonucleotides containing Gh or Sp[5,9] have shown that these lesions are highly mutagenic resulting in G → C and G → T transversion mutations.[27−31] The mutagenic consequences of oxidized DNA bases are mitigated in part by base excision repair (BER). The key players in BER are the DNA glycosylases, which are responsible for searching the genome for aberrant bases and initiating repair by extruding the damaged nucleobase from the helix and catalyzing N-glycosidic bond cleavage to release the modified base. The hydantoins Gh and Sp have been shown to be *in vitro* substrates for several BER glycosylases, including bacterial Fpg and Nei, Mimivirus (Mv) Nei1, and mammalian "Nei-like" (NEIL) enzymes.[32−40] The hydantoins Gh and Sp were previously shown to be excellent *in vitro* substrates for human glycosylase NEIL1.[1,36,41,42] In addition, the Sp lesion was detected in Nei deficient *Escherichia coli* cells treated with the potent oxidant chromate.[43] Together, this evidence suggests that the hydantoin lesions may be important substrates for BER *in vivo*. Surprisingly, analysis of the DNA mutational spectrum of

Received: June 13, 2013
Published: August 9, 2013

   dx.doi.org/10.1021/ja4059469 | J. Am. Chem. Soc. 2013, 135, 13851−13861

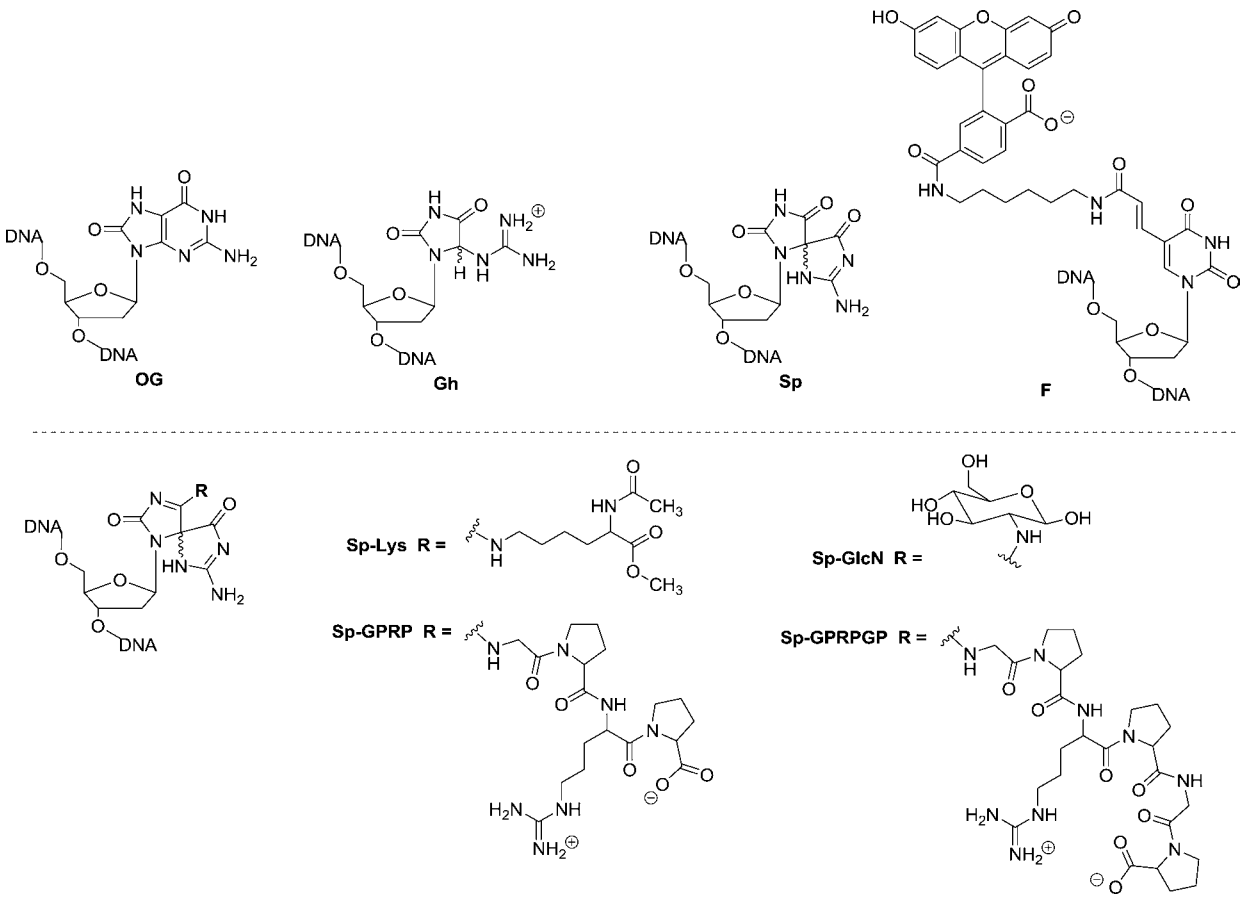

Figure 1. Structures of lesions used as substrates for NER and BER in this study.

lung tumors from *Neil1*$^{-/-}$ *Nth1*$^{-/-}$ mice was distinct from that expected for Gh and Sp, which suggests that there are alternative repair mechanisms for counteracting the mutagenicity of these lesions.[44]

An alternative pathway to consider for repair of hydantoins is nucleotide excision repair (NER). NER is known to repair bulky and helix-destabilizing DNA adducts such as *cis-syn* thymine−thymine cyclobutane dimers, DPC, and bulky alkylated bases.[45,46] The prokaryotic NER pathway is initiated by the UvrABC proteins, which respond in a coordinated fashion to locate the lesion and excise a lesion-containing oligonucleotide.[45,47,48] To delineate the contributions of NER and BER for hydantoin lesion repair, we prepared a series of Sp−amine adducts of varying size (Figure 1). The Sp−amine adducts used herein were designed to increase the size of the attached adduct and are derived from lysine, glucosamine, and short peptides. Our expectation was that the larger, more bulky Sp−amine adducts would be poor substrates for BER glycosylases but better substrates for the UvrABC complex. Single-turnover (STO) experiments with UvrABC revealed robust excision activity for the Sp−amine adduct-containing duplex DNA that was similar to that observed with the standard UvrABC substrate, a fluorescein-modified T (F).[49,50] Notably, the Sp and Gh lesions were also substrates for NER. The BER glycosylases Nei, Fpg, and NEIL1 were also shown to mediate the removal of Sp−amine adduct bases from DNA. Surprisingly, NEIL1 was able to cleave all Sp−amine adducts tested with rates comparable to that of the parent lesion Sp. Taken together, these results suggest that both repair pathways can mitigate the potent mutagenic properties of a diverse set of hydantoin lesions.

EXPERIMENTAL SECTION

General methods and procedures (reagents, instrumentation, enzyme purification, hydroxyl radical footprinting, and Maxam−Gilbert sequencing) are described in the Supporting Information.

Substrate DNA Preparation for NER Assays. The 50 bp duplex used in the incision assays was 5′-d(GAC TAC GTA CTG TTA CGG CTC CAT CXC TAC CGC AAT CAG GCC AGA TCTGC)·3′-d(CTG ATG CAT GAC AAT GCC GAG GTA GYG ATG GCG TTA GTC CGG TCT AGA CG), where X = OG, Gh, Sp, or F and Y = A, C, T, or G. Oligonucleotides [50 nucleotides (nt)] containing the lesions were generated by ligation of shorter oligonucleotides.[51] The oligonucleotides used for the ligation were 5′-d(GAC TAC GTA CTG TTA CG) and 5′-d(GCT CCA TCX CTA CCG CAA TCA GGC CAG ATC TGC), on the template strand 5′-d(TGG CCT GAT TGC GGT AGA GAT GGA GCC GTA ACA GTA).

The 51 bp duplex used in the incision assays had the sequence 5′-d(GAC TAC GTA CTG TTA CGG CTC CAT CXG CTA CCG CAA TCA GGC CAG ATC TGC)·3′-d(CTG ATG CAT GAC AAT GCC GAG GTA GYC GAT GGC GTT AGT CCG GTC TAG ACG), where X = Sp−Lys, Sp−GlcN, Sp−GPRP, or Sp−GPRPGP and Y = A, C, T, or G. The adducts were synthesized as follows. The 51 nt OG lesion strand (10 μM, 1 nmol) was mixed in the presence of the chosen primary amine (2 mM, 200 nmol) in a 20 mM sodium phosphate (pH 7.4) solution maintained at 45 °C. After a 30 min preincubation, the oxidation reaction was initiated by the addition of Na_2IrCl_6 (200 μM, 20 nmol) and the mixture incubated for an additional 30 min. The reaction was terminated by addition of Na_2EDTA (2 mM, 200 nmol). The mixtures were purified as described previously, and the identities of each adduct were determined by electrospray ionization mass spectrometry (ESI-

dx.doi.org/10.1021/ja4059469 | J. Am. Chem. Soc. 2013, 135, 13851−13861

MS).[25] UvrABC incision assays were conducted with both duplexes that contained the ^{32}P-labeled lesion (X)-containing strand. The X-containing strand (2.5 pmol) was radiolabeled either on the 5′-end using [γ-^{32}P]ATP with T4 kinase or on the 3′-end using [α-^{32}P]-cordycepin 5′-triphosphate with terminal transferase at 37 °C. The labeled strand was then annealed with a 10% excess of the complement by being heated to 90 °C for 10 min in annealing buffer [20 mM Tris-HCl (pH 7.6), 10 mM EDTA, and 150 mM NaCl] and then allowed to cool slowly overnight.

Substrate DNA Preparation for BER Assays. Gh-, Sp1-, Sp2-, and Sp-amine adduct-containing oligonucleotides were synthesized as described previously.[25,52] The duplex sequence used in the base excision assays was 5′-d(TGT TCA TCA TGC GTC XTC GGT ATA TCC CAT)·3′-d(ACA AGT AGT ACG CAG YAG CCA TAT AGG GTA), where X = Gh, Sp1, Sp2, or Sp-amine adduct (Sp−Lys, Sp−GlcN, Sp−GPRP, or Sp−GPRGP, respectively) and Y = A, C, G, or T. For glycosylase assays, the X-containing strand was 5′-end-labeled using [γ-^{32}P]ATP with T4 kinase and then mixed with unlabeled X-containing oligonucleotide to yield a solution that contained 5% labeled X-containing oligonucleotide. The mixture was then annealed with a 20% excess of the Y-containing complement strand by heating to 90 °C for 10 min in annealing buffer [20 mM Tris-HCl (pH 7.6), 10 mM EDTA, and 150 mM NaCl] and then cooling slowly overnight.

UvrABC Incision Assay. Single-turnover experiments, in which the enzyme concentration is greater than the DNA concentration, were performed to evaluate the incision activity of the UvrABC complex.[51,53] In each case, the final reaction volume was 100 μL with a final labeled DNA duplex concentration of 2 nM. The duplex was incubated with 20 nM UvrA, 100 nM UvrB, and 50 nM UvrC, in assay buffer [50 mM Tris-HCl (pH 7.5), 50 mM KCl, 10 mM $MgCl_2$, 5 mM DTT, and 1 mM ATP] at 55 °C. Before being added to the reaction mixture, the individual Uvr enzyme solutions were incubated for 10 min at 65 °C to activate the enzymes. Reaction time courses were initiated by addition of UvrC. Aliquots (8 μL) were taken at various time points ranging from 1 min to 4 h and reactions quenched by the addition of 2 μL of 100 mM EDTA (pH 8) and incubation at 90 °C for 5 min. Reaction mixtures were chilled on ice, and 10 μL of formamide denaturing dye (99.9% formamide, 0.025% xylene cyanol, and 0.025% bromophenol) was added prior to electrophoresis. The samples were electrophoresed on a 15% denaturing polyacrylamide gel in TBE running buffer [89 mM Tris-HCl, 89 mM boric acid, and 2 mM EDTA (pH 7.6)] at 800 V for 3 h to separate the DNA fragments arising from the cleaved product and the 50 or 51 nt substrate. The gel was visualized using storage phosphor autoradiography and quantitated using ImageQuant.

Base Excision Glycosylase Assays. Single-turnover (STO) experiments, in which the enzyme concentration was greater than the DNA concentration, were performed using the 30 bp duplex sequence to evaluate the glycosylase activity of BER glycosylases.[19,35,36,41,42,54] In all cases, the final reaction volume was 100 μL with a final DNA duplex concentration of 20 nM. In qualitative experiments to evaluate the glycosylases capable of excising Sp−amine adducts, the lesion-containing duplex was incubated with either 200 nM NEIL1, 200 nM Fpg, 200 nM E3Q Fpg, 200 nM Nei, 300 nM E3Q NEIL1, or 100 nM hOGG1 in assay buffer [20 mM Tris-HCl (pH 7.6), 10 mM EDTA, 0.1 mg/mL BSA, and NaCl (150 mM for NEIL1, 30 mM for Fpg, E3Q Fpg, and Nei, or 70 mM for hOGG1)] at 37 °C for 20 min. Enzyme concentrations are listed as active concentrations for NEIL1, Fpg, and hOGG1 and as total protein concentrations for Nei and E3Q NEIL1. For NEIL1 reactions under STO conditions, a rapid quench-flow (Kintek RQF-3) was utilized to determine kinetic parameters. The NEIL1 enzyme was mixed with 20 nM final DNA duplex for time points ranging from 0.2 s to 2 min and the reaction quenched with 2 μL of 0.5 M NaOH. Denaturing polyacrylamide gel electrophoresis (PAGE) provided separation of the 15 nt DNA fragment arising from the cleaved product and the 30 nt fragment originating from the substrate. Gels were imaged using storage phosphor autoradiography, and band intensities were quantified with ImageQuant to provide binding plots using GraFit version 5.0.

Gel Mobility Shift Assay. Electrophoretic mobility shift assays (EMSAs) were performed to determine the K_d values of UvrA for lesion-containing DNA.[53] For binding studies, the labeled lesion-containing strand was annealed to a complement DNA strand that positioned A opposite the lesion strand. Reaction mixtures (20 μL) contained 200 pM DNA duplex that was 5′-end-labeled with ^{32}P on the lesion-containing X strand in buffer [50 mM Tris-HCl (pH 7.5), 50 mM KCl, 10 mM $MgCl_2$, 5 mM DTT, and 1 mM ATP] and UvrA concentrations ranging from 0.5 to 200 nM. Samples of the protein/DNA mixture were incubated at 55 °C for 20 min followed by the addition of 2 μL of 80% glycerol. Bound versus unbound DNA was visualized using electrophoresis on a 4% nondenaturing poylacrylamide gel (80:1 acrylamide:bisacrylamide ratio) at room temperature in TBE running buffer (89 mM Tris, 89 mM boric acid, and 2 mM EDTA) containing 10 mM $MgCl_2$ and 1 mM ATP at 100 V for 2−3 h. Gels were dried and exposed to a storage phosphor screen overnight. K_d values were determined by fitting the data (percent bound substrate vs log[UvrA]) using a one-site binding isotherm (GraFit version 5.0). The K_d values were determined from data generated from at least three separate experiments (typically five) using separately diluted UvrA in each experiment.

The loading of UvrB by UvrA was examined by incubating the 5′-labeled DNA duplex (200 pM) with UvrA (0.5 nM) in the presence of 100 nM UvrB in buffer [50 mM Tris-HCl (pH 7.5), 50 mM KCl, 10 mM $MgCl_2$, 5 mM DTT, and 1 mM ATP] at 55 °C for 20 min. After addition of 2 μL of 80% glycerol, samples were electrophoresed on a 4% gel as described above.[53] The percent UvrB·DNA complex was determined from quantitation of the storage phosphor autoradiogram. At least three separate experiments were performed and the values averaged to provide the percent UvrB loaded onto the lesion-containing DNA.

RESULTS

Substrate Design, Synthesis, Purification, and Characterization. Insight into the biological consequences of Gh and Sp lesions has emerged in part because of the ability to synthesize DNA oligonucleotides containing these lesions at a defined location by oxidation of OG with the one-electron oxidant sodium hexachloroiridate(IV).[5,9] Appropriate oxidation conditions were used to produce oligonucleotides containing primarily Gh or Sp; subsequent separation of the desired lesion oligonucleotide from other products was performed using high-performance liquid chromatography (HPLC).[52] A 33 nt fragment was used for the Ir(IV) oxidation reaction to make the Gh- or Sp-containing oligonucleotide that was then ligated to a 17 nt strand using a 36 nt complement sequence as a template.[51] In this 33 nt sequence, the two diastereomers of Sp could not be separated via HPLC, and therefore, the duplex substrates containing Sp are a mixture of diastereomers. The overall yields of the ligation and purification of the 50 nt strands containing OG, Gh, and Sp were 50, 20, and 10%, respectively. After gel purification, the ligated 50 nt product was annealed to the appropriate 50 nt complement strand to position the lesion opposite C, G, A, or T. The Sp−amine adduct-containing DNA duplexes were generated by Ir(IV) oxidation of a 51 nt strand containing a central OG lesion in the presence of the chosen primary amine. The amines were selected to be biologically relevant water-soluble amines, such as glucosamine, lysine, and short peptides. The peptide sequences featured an N-terminal amino group to serve as the nucleophile and rigid, bulky components (proline) as well as arginine for enhanced water solubility and DNA affinity. Spermine and spermidine adducts were previously synthesized; however, these adducts undergo intramolecular rearrangement and decomposition reactions, making them unsuitable choices for the studies reported here.[23] HPLC purification was used to

separate the amine adduct from other products as a mixture of diastereomers. The identity for each adduct was determined by ESI-MS: 51-mer OG (calcd mass of 15612.2 Da, exptl mass of 15612.8 Da), 51-mer Sp−Lys (calcd mass of 15813.9 Da, exptl mass of 15812.8 Da), 51-mer Sp−GlcN (calcd mass of 15789.3 Da, exptl mass of 15788.8 Da), 51-mer Sp−GPRP (calcd mass of 16034.7 Da, exptl mass of 16035.2 Da), and 51-mer Sp−GPRPGP (calcd mass of 16188.8 Da, exptl mass of 16189.6 Da).

Incision Activity of UvrABC with DNA Substrates Containing OG−, Gh−, Sp−, F−, and Sp−Amine Adducts. The incision activity of the UvrABC complex was evaluated using recombinant *Bacillus caldotenax* UvrA and UvrB and *Thermatoga maritima* UvrC enzymes with duplex substrates containing the lesion X (X = OG, Gh, Sp, F, Sp−Lys, Sp−GlcN, Sp−GPRP, or Sp−GPRPGP) paired with all four natural bases (A, G, C, and T). The general method involved 5′-end-labeling the X-containing strand using [γ-^{32}P]ATP to monitor the extent of excision 5′ to the X nucleotide. Alternatively, 3′-end-labeling of the X-containing strand was achieved with [α-^{32}P]cordycepin 5′-triphosphate to monitor the cleavage 3′ to the X nucleotide. Reactions were performed under STO conditions, where the enzyme concentration is greater than the DNA concentration, and the data were fit to a single-exponential equation to determine the observed rate of product formation as a function of time (k_{obs}). The excision activity of UvrABC with Gh, Sp, the Sp−amine adducts, and OG was compared to that with the standard NER substrate, fluorescein-dT (F)-containing DNA, and the conditions were optimized to give maximal levels of excision similar to that reported previously.[51,53,55] Representative reaction progress curves for the lesions base-paired with A are shown in Figure 2. The

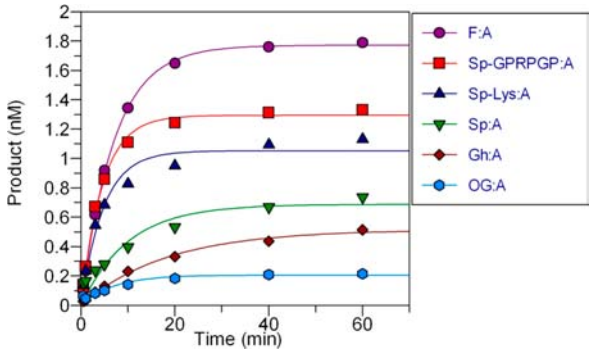

Figure 2. Representative reaction profiles of UvrABC with hydantoin lesion-containing DNA. Reaction conditions consisted of 20 nM UvrA, 100 nM UvrB, 50 nM UvrC, and 2 nM DNA duplex in assay buffer [50 mM Tris-HCl (pH 7.5), 50 mM KCl, 10 mM $MgCl_2$, 5 mM DTT, and 1 mM ATP] at 55 °C. Reactions and plots with UvrABC and DNA containing Sp−GPRP:A and Sp−GlcN:A were essentially identical to the reaction with Sp−GPRPGP:A.

observed rates of product formation as a function of time for the reaction of UvrABC with all lesion:A-containing duplexes and the control F:A-containing duplex were found to be similar (0.2 ± 0.1 min^{-1}) (Table 1). However, distinct differences were observed with respect to the maximal amount of excision mediated by UvrABC with the series of lesion:A-containing duplexes. Indeed, the reaction proceeded to 88 ± 2% product formation with the fluorescein-containing duplex, whereas experiments using Gh and Sp reached 23 ± 4 and 32 ± 3% completion after 4 h, respectively. In contrast, the reactions

Table 1. Observed Rates (k_{obs}) and Extents of Product Formed in STO Reactions (percent) with UvrABC, Equilibrium Dissociation Constants (K_d) Determined for UvrA, and Fractions of the UvrB DNA Complex (percent) with Lesion-Containing Duplexes[a]

base pair	k_{obs} (min^{-1})[b]	product formed under STO conditions (%)	K_d (nM)[c]	DNA bound in a stable complex with UvrB (%)[d]
F:A	0.2 ± 0.1	88 ± 2	7 ± 5	81 ± 7
Sp:A	0.1 ± 0.1	32 ± 3	13 ± 7	9 ± 4
Gh:A	0.1 ± 0.1	23 ± 4	20 ± 10	7 ± 3
OG:A	0.1 ± 0.1	10 ± 1	23 ± 7	5 ± 2
Sp−Lys:A	0.2 ± 0.1	51 ± 1	2 ± 1	38 ± 2
Sp−GlcN:A	0.2 ± 0.1	62 ± 4	3 ± 1	22 ± 1
Sp−GPRP:A	0.2 ± 0.1	62 ± 3	2 ± 1	54 ± 1
Sp−GPRPGP:A	0.2 ± 0.1	62 ± 4	2 ± 1	61 ± 5

[a]Errors are standard deviations of the average of at least three reactions. [b]k_{obs} determined using a single-exponential rate equation at 55 °C. [c]K_d values and percent DNA bound by UvrB determined using an EMSA at 55 °C (see the Experimental Section). [d]DNA bound by UvrB (percent) determined by gel quantitation with 0.5 nM UvrA.

with OG reached only 10 ± 1% completion. Excision reactions with the Sp−amine adducts Sp−Lys, Sp−GlcN, Sp−GPRP, and Sp−GPRPGP proceeded to 51 ± 1, 62 ± 4, 62 ± 3, and 62 ± 4% completion, respectively. The extents of product formation and the observed rates of the Sp−amine adducts, F, Gh, Sp, and OG from all possible natural base pair contexts were within error for each lesion (data not shown), indicating a lack of preference for the opposite base during UvrABC substrate processing. Although the rates of incision are similar for OG, F, and all hydantoin lesions, a comparison of the maximal extent of substrate cleavage reveals that the Sp−amine adducts are good substrates for UvrABC. Indeed, the extents of Sp−amine adduct removal are similar to that reported for excision of DNA−peptide cross-links by UvrABC.[55]

To determine the sites of UvrABC backbone cleavage relative to the lesion, the bands for UvrABC incision were compared to Maxam−Gilbert G + A sequencing reactions (Figure 3A−C).[54,56] These experiments were performed using both 5′- and 3′-end-labeled duplex. In the case of the 3′-labeling, the UvrABC incision site maps the most closely to C30, which is located four nucleotides from the lesion. In the case of the 5′-incision site, the UvrABC product band appears between C19 and T20 in the Maxam−Gilbert sequencing lane likely because of the presence of a phosphate end in the latter. Because of the slower migration of a DNA fragment with a hydroxyl end versus a phosphate end, the cleavage site for UvrABC was assigned to the phosphodiester 5′ of C19. Importantly, the site of phosphodiester backbone cleavage by UvrABC both 5′ and 3′ to the lesion was the same with F, OG, Gh, Sp, and the Sp−amine adducts (Figure 1 of the Supporting Information).

Equilibrium Dissociation Constants (K_d) of UvrA with Lesion-Containing DNA. Prokaryotic NER is initiated by UvrA, which forms a heterotetramer with UvrB ($UvrA_2$·$UvrB_2$) to locate and bind damaged DNA.[45,57−60] To determine if the reduced amount of product formation for the hydantoin lesions and OG relative to that of the fluorescein standard substrate was due to inefficient recognition of the lesion base by UvrA, EMSAs were employed to determine the equilibrium

dx.doi.org/10.1021/ja4059469 | J. Am. Chem. Soc. 2013, 135, 13851−13861

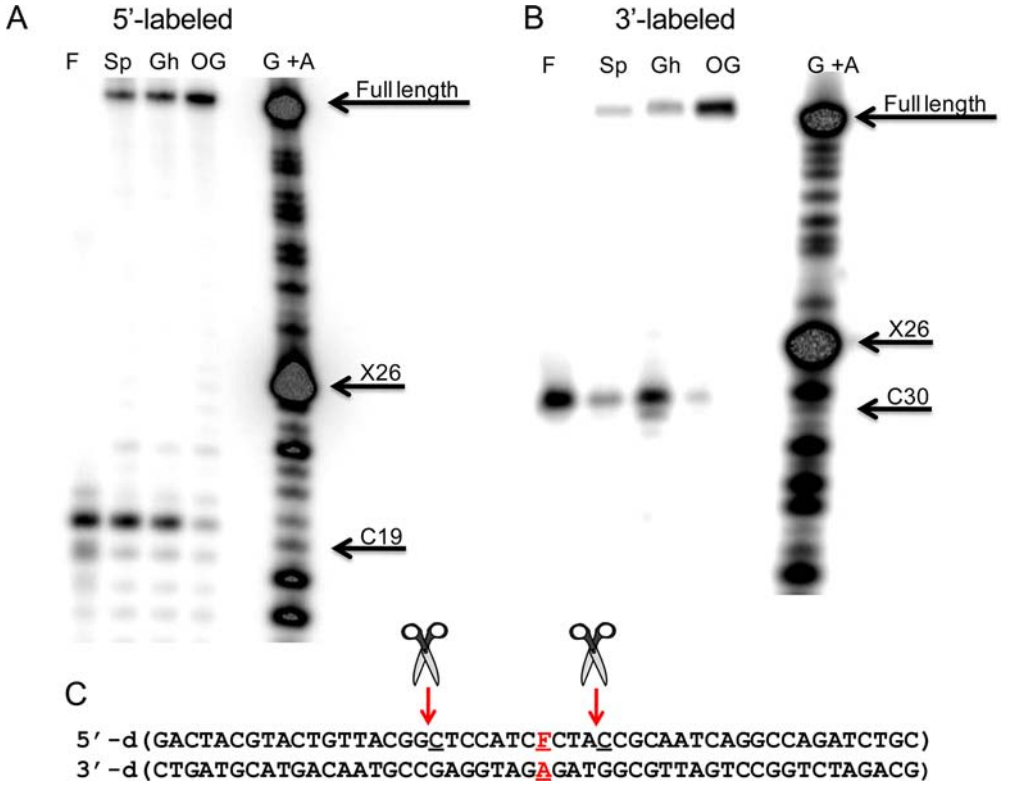

Figure 3. Location of UvrABC incision sites near the lesion site. (A) Storage phosphor autoradiogram of the UvrABC 5′-side incision site on [5′-^{32}P]F-, -OG-, -Gh-, or -Sp-containing strand of the 50 bp duplex substrate. The Maxam−Gilbert G + A sequencing reaction (lane G + A) was used to determine the location of the lesion site (X26) and the nucleotide cleaved by UvrABC (C19). Reaction mixtures containing 2 nM DNA duplex with 20 nM UvrA, 100 nM UvrB, and 50 nM UvrC were incubated for 4 h at 55 °C. (B) Storage phosphor autoradiograph of the same experiment using 3′-end-labeling to visualize the 3′-cleavage site. Highlighted nucleotides are the lesion site (X26) and the UvrABC 3′-incision site (C30). (C) Sequence of the 50 bp duplex containing F:A with nucleotides that are hydrolyzed by UvrABC indicated with arrows and scissors. Sites of UvrABC incision were the same for all lesion-containing duplexes.

dissociation constants (K_d) (Figure 2 of the Supporting Information). EMSA analysis was performed under conditions where the DNA duplex concentration was less than the K_d. The DNA−UvrA complex concentration was determined as a function of the UvrA concentration, and the data were fit using a one-site binding isotherm. UvrA binding experiments conducted with lesion-containing oligonucleotides revealed that UvrA recognizes and binds F, Gh, Sp, OG, and the Sp−amine adducts when base paired to adenine (Table 1). The K_d of UvrA for fluorescein-containing DNA was determined to be 7 ± 5 nM. The K_d values of UvrA for Gh- and Sp-containing duplexes were 20 ± 10 and 13 ± 7 nM, respectively, while the K_d value of UvrA for OG-containing DNA was found to be 23 ± 7 nM. UvrA was shown to possess the highest binding affinity for the Sp−amine adducts in which the following values were determined: 2 ± 1 nM for Sp−Lys, 3 ± 1 nM for Sp−GlcN, 2 ± 1 nM for Sp−GPRP, and 2 ± 1 nM for Sp−GPRPGP. However, the measured K_d values for the Sp−amine adducts were all within error of that of the fluorescein−dT adduct.

Formation of the UvrB·DNA Preincision Complex Measured via an EMSA. The loading of UvrB onto the site of damage by UvrA and the formation of the stable UvrB·DNA preincision complex are important steps in the damage repair mechanism of NER.[45] The UvrB·DNA preincision complex recruits UvrC to conduct the 5′- and 3′-incision to remove the damaged DNA fragment. The extent of formation of a stable UvrB hydantoin-containing DNA complex was evaluated using an EMSA. Failure to form a stable UvrB·DNA preincision complex despite successful UvrA recognition may be the cause of the reduced level of UvrABC-mediated excision observed with Gh, Sp, and OG substrates relative to that with F. An EMSA was performed in the presence of 100 nM UvrB, using a low concentration of the DNA duplex (below the K_d for UvrA) to examine the formation of the DNA·UvrB complex as a function of UvrA concentration. Efficient formation of the UvrB·DNA preincision complex was detected with F:A base pair-containing DNA (81 ± 7% DNA bound) even at the lowest concentrations of UvrA (0.5 nM) (Figure 4). Using this concentration of UvrA, a reduced level of formation of the UvrB·DNA preincision complex was observed with Gh (7 ± 3%) and Sp (9 ± 4%). Similarly, a small fraction of OG-containing DNA (5 ± 2%) was bound to UvrB under these same conditions. Significantly larger amounts of the UvrB·DNA preincision complex were detected with Sp−Lys (38 ± 2%), Sp−GlcN (22 ± 2%), Sp−GPRP (54 ± 2%), and Sp−GPRPGP (61 ± 5%) than with OG, Gh, and Sp. The extent of the UvrB lesion·DNA complex observed via an EMSA indicates the efficiency of loading of UvrB onto DNA and formation of a stable complex. Notably, the amount of the UvrB·DNA complex observed with OG, Gh, and Sp-containing DNA relative to that observed with Sp−GlcN, Sp−Lys, Sp−GPRP, Sp−GPRPGP, and F correlates well with the extent of product formation from the UvrABC incision assay experiments.

Activity of BER Glycosylases with DNA Substrates Containing Gh, Sp1, Sp2, and Bulky Sp−Amine Adducts.

dx.doi.org/10.1021/ja4059469 | J. Am. Chem. Soc. 2013, 135, 13851−13861

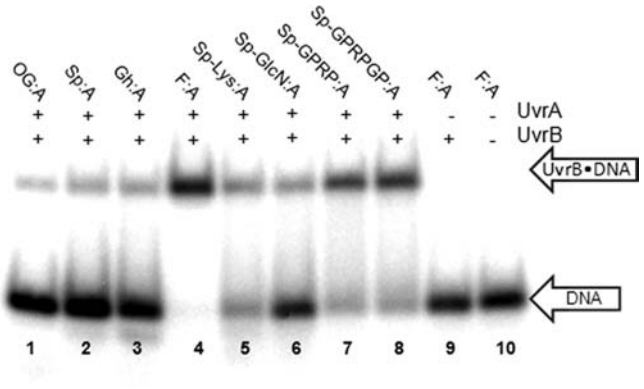

Figure 4. Representative EMSA storage phosphor autoradiogram illustrating the formation of the UvrB·DNA preincision complex with F, OG, Gh, Sp, and Sp−amine adducts containing DNA. Reaction mixtures contained 200 pM DNA duplex, 100 nM UvrB, 0.5 nM UvrA, 50 mM Tris-HCl (pH 7.5), 50 mM KCl, 10 mM $MgCl_2$, 5 mM DTT, and 1 mM ATP and were incubated at 55 °C for 20 min.

The glycosylase activity of Nei, Fpg, E3Q Fpg, hOGG1, NEIL1, and E3Q NEIL1 was evaluated using STO conditions ([E] > [DNA substrate]) with a 30 bp duplex containing Gh, Sp1, Sp2, Sp−Lys, Sp−GlcN, or Sp−GPRPGP lesions base paired to C at a single time point of 20 min (Figure 5). The reactions were performed in a manner similar to that previously published.[35,36,42,54,61] Briefly, the protocol involved 5′-end-labeling the X-containing strand with [γ-^{32}P]ATP and resolution of reaction products with denaturing PAGE to quantify the extent of strand cleavage at the X nucleotide after quenching with 0.5 M NaOH. The base treatment ensured that cleavage of the phosphodiester backbone occurred at all abasic sites produced by the glycosylase.[36] These experiments revealed that Nei, Fpg, and NEIL1 were able to remove the Sp−amine adducts while the hOGG1 glycosylase exhibits minimal activity for Gh, Sp1, Sp2, or the Sp−amine adducts above background levels (Figure 5). The catalytically inactive variants E3Q Fpg and E3Q NEIL1 were unable to mediate base release, confirming the requirement for enzyme catalysis of N-glycosidic bond cleavage.

Measurements of the rate of base removal mediated by Fpg under STO conditions showed a decrease in rate of 4−5-fold for the Sp−amine adducts compared to that with Sp alone (Figure 3 of the Supporting Information). In contrast, manual glycosylase assays for removal of Sp−amine adducts and Sp by NEIL1 indicated that the reactions were complete at the first time point (20 s). Initial experiments used edited NEIL1 (Arg at position 242), which is the form of NEIL1 most commonly studied.[41] However, because of previous work that has shown differences in activity between edited and unedited NEIL1 (Lys at position 242),[41] a more detailed analysis was conducted with both enzyme forms using STO conditions with a 30 bp duplex containing the lesion (Gh, Sp1, Sp2, Sp−Lys, Sp−GlcN, or Sp−GPRP) in all four possible natural base pairing contexts (Table 2 and Tables 1 and 2 of the Supporting Information). Strand cleavage was monitored using a rapid quench-flow instrument, and the resulting progress curves were fit to either a single- or double-exponential equation to determine rates for the glycosylase reactions. The measured rates for removal of Gh, Sp1, and Sp2 follow the previously reported trend for a different 30 bp sequence, in which all three hydantoin lesions are excellent substrates for both NEIL1 isoforms.[36] Of the three lesions, Sp1 was the most rapidly removed diastereomer.

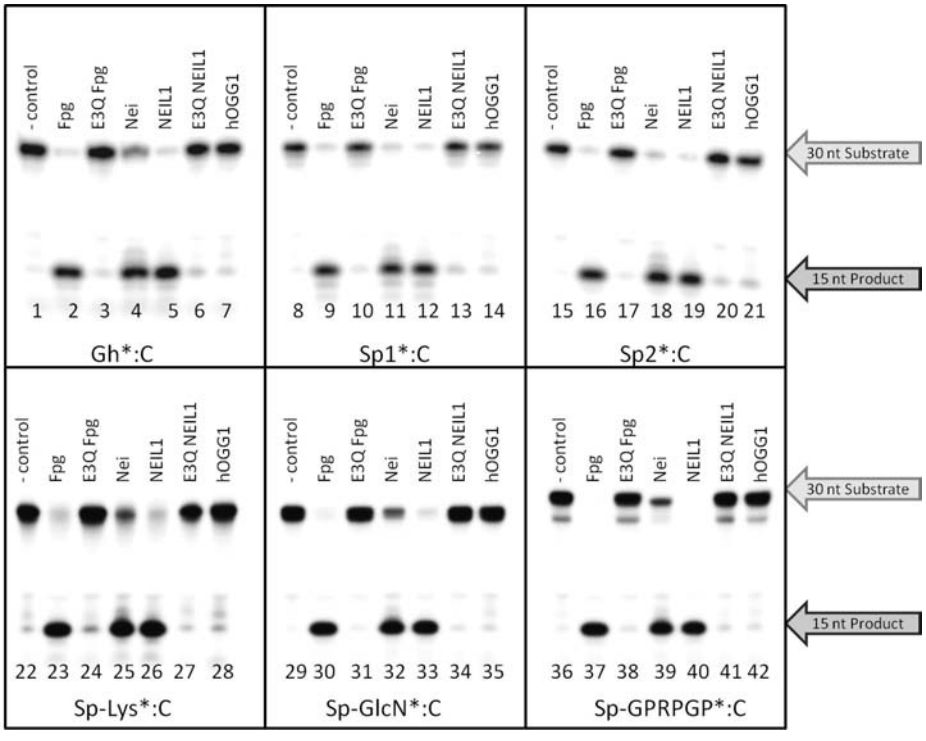

Figure 5. Sp−amine adduct removal by human and bacterial BER glycosylases. Qualitative glycosylase assays were performed with Fpg, E3Q Fpg, Nei, NEIL1, E3Q NEIL1, and hOGG1 using the 30 bp duplex containing Gh, Sp1, Sp2, Sp−Lys, Sp−GlcN, and Sp−GPRPGP lesions base paired to C.[35,36,54,61] The asterisk indicates the lesion-containing strand containing the [5′-^{32}P]phosphate. The enzyme reactions were performed at 37 °C, and the reactions were quenched with 0.5 M NaOH after 20 min. The Sp−GPRPGP oligonucleotide degraded slightly to approximately 3% Sp, which is evident in the slightly faster mobility in the substrate band (lanes 36−42).

dx.doi.org/10.1021/ja4059469 | J. Am. Chem. Soc. 2013, 135, 13851−13861

Table 2. Rate Constants for NEIL1 with Hydantoins Determined under Single-Turnover Conditions[a]

base pair	k_g' (min^{-1})	k_g'' (min^{-1})
Spl:A	320 ± 30	NA[b]
Sp2:A	47 ± 5	NA[b]
Gh:A	130 ± 10	NA[b]
Sp−Lys:A	370 ± 70	7 ± 1
Sp−GlcN:A	210 ± 90	3 ± 1
Sp−GPRP:A	330 ± 80	9 ± 2

[a]Rate constants determined at 37 °C under STO conditions with hydantoin lesions base paired to A in a 30 bp duplex. Reactions proceeded to >75% completion. Data for Sp−amine adducts were fit with a double-exponential model generating k_g' and k_g''. Errors are standard deviations of the average of at least three independent trials. The capacity represents the percentage of each rate in the double-rate fits and the capacity for k_g' is 50 ± 2% for Sp−Lys:A, 41 ± 2% for Sp−GlcN:A, and 36 ± 2% for Sp−GPRP:A and for k_g'' is 50 ± 2% for Sp−Lys:A, 59 ± 2% for Sp−GlcN:A, and 64 ± 2% for Sp−GPRP:A. [b]Not applicable.

Remarkably, all bulky Sp−amine adduct lesions in all base pair contexts were removed efficiently by both isoforms of NEIL1 (edited and nonedited). In most base pair contexts, the reactions were processed at such a high rate (>500 min^{-1}) that it was only possible to estimate a lower limit. A complete table of kinetic values for the glycosylase activity with the lesions used in this work in all base pair contexts is available in Tables 1 and 2 of the Supporting Information. Base excision by edited NEIL1 from duplex substrates containing the hydantoin lesion paired with A yielded experimentally accessible rate limits, and therefore, measurable rate constants for removal of Sp−Lys (370 ± 70 min^{-1}), Sp−GlcN (210 ± 90 min^{-1}), and Sp−GPRP (330 ± 80 min^{-1}) that are on the same order of magnitude as the rate of removal of Sp1 in the corresponding duplex substrate (320 ± 30 min^{-1}) were determined. Representative reaction profiles for edited NEIL1 with DNA duplexes containing Sp1:A and Sp−GPRP:A are shown in Figure 4 of the Supporting Information, and the rate constants for Sp1:A, Sp2:A, Gh:A, Sp−Lys:A, Sp−GlcN:A, and Sp−GPRP:A are listed in Table 2.

Hydroxyl Radical Footprinting with E3Q NEIL1. Hydroxyl radical footprinting was used to define the contact region of the catalytically inactive E3Q NEIL1 protein on both the lesion and complementary strand of the DNA duplex. Hydroxyl radicals were generated using Fe(II)·EDTA to initiate 2′-deoxyribose cleavage in a manner similar to that previously reported by our laboratory.[35] The 30 bp duplexes containing Gh, Sp1, Sp2, Sp−Lys, Sp−GlcN, and Sp−GPRPGP lesions paired with G or A were incubated with increasing amounts of E3Q NEIL1 followed by addition of Fe(II)·EDTA. In each case, either the lesion-containing strand or the complementary strand contained a [5′-^{32}P]phosphate label. The end-labeled oligonucleotides were also subjected to Maxam−Gilbert G + A sequencing to determine the nucleotides that were protected by E3Q NEIL1−DNA interactions. Representative storage phosphor autoradiograms for the footprinting experiments with E3Q NEIL1 with Sp−GlcN:G-containing DNA and a histogram showing the extent of protection at specific nucleotides are shown in Figures 5 and 6 of the Supporting Information. In each case, a protected region was observed in the presence of the enzyme that spans approximately 17−20 nucleotides on both strands of the DNA duplex, regardless of the lesion identity or the base pair context. The protection from hydroxyl radical cleavage provided by E3Q NEIL1 on the G-containing strand is much more modest than that on the lesion-containing strand, suggesting more localization of the enzyme on the lesion strand. Notably, there was an increase in the extent of hydroxyl radical cleavage of the deoxyribose of the lesion nucleotide (2.4-fold) as well as a G nucleotide 5 bp 5′ of the lesion in the presence of E3Q NEIL1. This enzyme-induced hyperreactivity at the lesion site and nearby suggests an increased degree of access to the hydroxyl radical upon formation of the E3Q NEIL1−DNA complex.

DISCUSSION

NER typically targets large bulky lesions, whereas BER is generally entrusted to repair more subtle base modifications. However, the work presented here with the UvrABC proteins shows that NER is able to recognize the bulky Sp−amine adducts quite efficiently but also effectively acts on the small hydantoin lesions Gh and Sp. Remarkably, this work also demonstrates that the BER glycosylase NEIL1 is capable additionally of removing large and bulky Sp−amine base modifications as efficiently as the small parent lesion Sp. Indeed, despite the distinct mechanisms of DNA repair of NER and BER, this work underscores the similarity in the mechanisms used to recognize a diverse set of damaged DNA substrates. Moreover, the overlapping mechanisms targeting hydantoin and hydantoin−amine adducts are likely important for ensuring the removal of these potently mutagenic and toxic lesions.

Our studies revealed that the UvrABC system excises the small base lesions, Gh, Sp, and OG, as well as the large Sp−amine adducts. Similar rates of excision were measured for all substrates tested; however, the overall level of excised product differed among the lesion-containing substrates. Fluorescein-adducted dT, which served as a control for an excellent substrate, was the most efficiently processed substrate with reactions proceeding nearly to completion (88 ± 2%). The Sp−amine adducts were also efficiently processed with reactions reaching ∼60% completion, suggesting that the more bulky Sp−amine adducts are the most preferred hydantoin lesions for repair via NER. The difference in the amount of excised product did not correlate with binding of UvrA to the lesion duplex based on the similar equilibrium dissociation constants (K_d) measured for UvrA with all of the damaged substrates. Notably, however, the extent of formation of a stable UvrB·DNA preincision complex correlated with the level of lesion excision, with a smaller fraction of UvrB bound to the more poorly processed substrates OG, Gh, and Sp than the more efficiently processed substrates F, Sp−GlcN, Sp−Lys, Sp−GPRP, and Sp−GPRPGP. These results are consistent with the known sequence of events in NER that requires initial lesion duplex binding by UvrA followed by recruitment of UvrB to form the preincision complex.[57,58,60] The preincision complex with UvrB recruits UvrC to catalyze the phosphodiester incision 5′ and 3′ to the lesion. We suggest that the formation of the stable preincision complex is the limiting factor in determining the fraction of substrate converted to product, and this process is sensitive to the type of lesion.[45] However, once the UvrB·DNA complex is formed, recruited UvrC mediates phosphodiester cleavage at a similar rate regardless of the identity of the lesion.

The ability to effectively recognize these structurally related lesions that differ considerably in size highlights the flexible damage recognition mechanism of NER.[45] Most studies suggest

dx.doi.org/10.1021/ja4059469 | J. Am. Chem. Soc. 2013, 135, 13851−13861

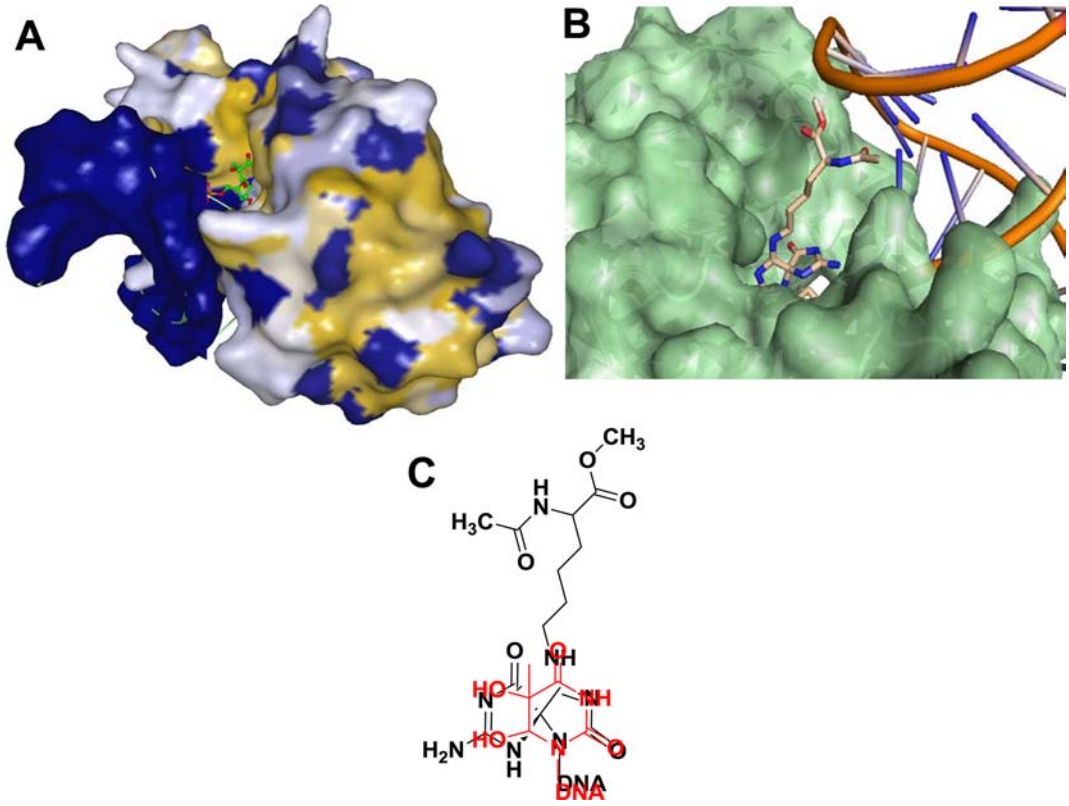

Figure 6. Structural rationale for potent activity of NEIL1 on Sp−amine adducts. (A) Structure of E3Q MvNei1 bound to Tg-containing DNA. The enzyme−DNA structure surface is mapped according to hydrophobicity [ranging from yellow (high) to blue (low)], with the Tg structure shown as a ball and stick model. The enzyme has very few amino acid interactions with the Tg lesion, which appears to be solvent-exposed. (B) Modeled *S*-Sp−Lys in the active site: A ring of Sp−Lys in an orientation similar to that of Tg and the B ring and Lys adduct accommodated in the open space at the back of the binding pocket. (C) Structure of Tg (red) overlaid on the structure of the Sp−Lys adduct. Panels A and B were generated using the MvNei−Tg structure from the Protein Data Bank (entry 3VK8) reported by Doublie and co-workers.[81]

that the thermodynamic destabilization of B-form DNA induced by lesions is an important factor in both prokaryotic and eukaryotic NER processing.[62] Previous work has shown that insertion of a β-hairpin motif of UvrB into the DNA duplex facilitates the ATPase activity of UvrB, and its associated helicase activity, which allows UvrB to take possession of the lesion from UvrA and to locate the lesion on the correct strand.[63,64] It is believed that the lesion-containing strand is captured underneath the β-hairpin, in which the base 3′ to the damaged nucleotide is flipped into a highly conserved nucleotide-binding pocket in the process of forming the UvrB preincision complex.[65,66] The stability of the UvrB·DNA preincision complex is likely connected to the ease of insertion of the β-hairpin into the duplex at the site of damage, aided by base stacking interactions with key tyrosine residues, which in turn is modulated by the structural and thermodynamic features of the lesion-containing duplex.[62] Our results are consistent with this proposal: reduced activity and formation of the UvrB·DNA preincision complex were noted for OG, a planar, non-helix-distorting lesion compared to the nonplanar, helix-destabilizing spirocyclic Sp and its amine adducts.[29,67,68] Accommodating the Sp−amine adducts within the DNA duplex would be expected to require widening of the duplex and perturbations in both DNA base stacking and base pairing that result in lower duplex stability.[67,69] The compromised local base pair stability would facilitate insertion of the β-hairpin by UvrB into the DNA duplex and subsequent capture of the damaged DNA strand by the active site.

This work also establishes that the Sp−amine adducts are substrates for bacterial BER glycosylases Nei and Fpg and the human BER glycosylase NEIL1. In the case of Fpg, the efficiency of removal of the Sp−amine adducts was reduced relative to that observed for the parent lesion Sp. In contrast, the Sp−amine adducts are removed from duplex DNA at rates similar to those with Gh, Sp1, and Sp2, for both edited and nonedited NEIL1. This underscores the fact that the Sp−amine adducts, despite their steric bulk, are excellent substrates for NEIL1. These new hydantoin substrates join an already broad list of substrates that have been identified for NEIL1.[70] Of the oxidized bases removed by NEIL1, 2,6-diamino-4-hydroxy-5-formamidopyrimidine (FapyG) and 4,6-diamino-5-formamido-pyrimidine (FapyA) are well-established substrates for NEIL1.[44,71−74] Oxidized pyrimidines such as thymine glycol (Tg) and 5-hydroxyuracil (5-OHU) are also removed by NEIL1; however, notably, NEIL1 shows little activity toward OG.[34,36,41,73,75−77] In addition to small base lesions, NEIL1 has been shown to remove bulky psoralen−base adducts, as well as psoralen-induced interstrand cross-links in three-stranded DNA structures.[78,79] Importantly, this work shows quantitatively that the extent of removal of large Sp−amine adducts is similar to that of the parent Sp lesion. These results suggest that the NEIL1 active site is flexible and open to accommodate large adducts to the base and efficiently remove them.

In the analysis of the glycosylase assays of NEIL1 with the amine adducts (e.g., Sp−Lys), the data fit better to a double-exponential equation with two distinct rates. These two

different rates are likely due to differential rates of processing of the two Sp−amine adduct diastereomers. We have previously shown that NEIL1 preferentially removes one diastereomer (Sp1 over Sp2) relative to the other.[36] The large attached amine may be more readily accommodated in the orientation presented by one diastereomer than the other. The preferred *anti*/*syn* glycosidic bond orientation and the influence of the opposite base pair would also be expected to be distinct for the two diastereomers.[29,67,69,80] Indeed, a slower rate of processing of all of the hydantoin lesions was observed in base-pairing contexts with A relative to C. The influence of the opposite base with NEIL1 may be indirect by influencing base pair stability or lesion conformation.

Recently, the first cocrystal structures of Mimivirus Nei1 (MvNei1), a viral ortholog of NEIL1, bound to damage-containing DNA were elucidated.[81] Examination of the X-ray structure of the complex of an inactive variant of E3Q MvNei1 bound to a thymine glycol (Tg)-containing duplex shows that the C5 and C6 positions of Tg are solvent-exposed, with only water-mediated amino acid interactions (Figure 6A). To provide insight into how a glycosylase (e.g., NEIL1) may be able to recognize bulky Sp−amine adducts, a structure was generated in which *S*-Sp−Lys was modeled into the active site of this lesion-containing MvNei1 structure (Figure 6B). The modeled Sp−Lys was positioned so the "pseudo-thymine" A ring of Sp−Lys would overlap with the oxidized pyrimidine ring of Tg (Figure 6C). This model reveals that the A ring of Sp−Lys can orient in a position similar to that of the Tg, allowing the B ring of Sp−Lys and the lysine chain of the adduct to be accommodated in the open space of the complex. This model suggests that despite their significant bulk, Sp−amine adducts may be easily accommodated in the MvNei1 (and presumably NEIL1) active site. Consistent with this model, Fe(II)·EDTA footprinting experiments using the catalytically inactive E3Q NEIL1 demonstrated the increased reactivity of the hydantoin lesion nucleotide with hydroxyl radicals, suggesting increased accessibility of the nucleotide sugar to the hydroxyl radical in the presence of the enzyme.[35]

Interestingly, the crystal structures of E3Q MvNei1 bound to duplex DNA containing Tg or 5-hydroxyuracil (5-OHU) exhibit minimal protein amino acid interactions with the pyrimidine lesions in the lesion binding site.[81] In fact, 5-OHU was found to adopt both *anti* or *syn* glycosidic bond orientations, suggesting minimal stabilization of the lesion in the active site. Additionally, the authors confirmed that mutation of two amino acid residues that make contacts with the lesion base (E6A and Y253F) did not significantly reduce glycosylase activity, revealing that these amino acids are not strictly required for the removal of aberrant bases. The authors replaced the Tg in the E3Q MvNeil−Tg structure with an undamaged T to illustrate that lack of obvious amino acid interactions in the active site to provide for discrimination for the damaged base. Because MvNei1 does not cleave thymine, this suggests that MvNei1 uses an alternative method to recognize substrates prior to the base flipping into the active site. These observations taken together suggested that this crystal structure captures a glimpse of a step that is subsequent to the one allowing for discrimination between damaged and undamaged DNA bases. The results suggest that key features of damage recognition by this glycosylase involve sensing local conformational distortions in the phosphodiester backbone and base pair stability. Notably, these damage recognition features are reminiscent of those used in the NER pathway.

The ability of NEIL1 to process large Sp−peptide adducts suggests that NEIL1 may be capable of excising DPC formed via oxidative reactions. Hydantoin−protein cross-links can be generated from oxidation with numerous biologically relevant oxidants in the presence of DNA binding proteins.[21,22,25,26] The mechanism of repair of DPC may involve proteolytic digestion to aid in removal of the majority of the protein adduct followed by repair initiated by NER, BER, or cooperation between the two pathways.[46,55,82−85] In addition, NEIL1 has been suggested to influence NER-mediated repair of (5′*R*)- and (5′*S*)-8,5′-cyclo-2′-deoxyadenosine lesions based on accumulation of these NER substrates in *Neil1*$^{-/-}$ mice.[86] Because NEIL1 is not capable of cleaving these cyclopurine adducts, NEIL1 was postulated to play a role in the initial lesion recognition and recruitment of NER.[86] Of note, cells from patients with Cockayne's syndrome (CS) have been shown to have a weakened ability to repair OG, 8-oxo-7,8-dihydroadenine (OA), and Tg base lesions generated during oxidative stress.[87−92] This finding was surprising because the mutated genes associated with CS (CSA and CSB) encode two transcription-coupled repair NER-specific factors.[93,94] It has also been shown *in vitro* that CSB stimulates NEIL1 glycosylase activity, and that CSB and NEIL1 co-immunoprecipitate and colocalize in HeLa cells. These results suggest that defective interactions between the mutant Cockayne syndrome NER proteins and the BER glycosylase NEIL1 may be involved in the pathogenesis of CS.[87] These observations, taken together with the overlapping substrate spectrum of the two repair pathways, suggest that coordination events between NER and BER may be critical for the preservation of the genome.

■ CONCLUSION

We have demonstrated that the helix-distorting hydantoin lesions derived from guanine oxidation, as well as their amine-adducted structures, are substrates for both the BER and NER pathways. Even though hydantoin lesions are present at low concentrations compared to that of OG, their high mutagenic potential and ability to stall replication forks and induce strand slippage make their presence in cells more detrimental than the presence of OG. Moreover, Sp−amine adduct-containing DNA−protein cross-links would be expected to be extremely toxic to cells.[2] Undoubtedly, the maintenance of genomic integrity and cell survival requires efficient repair of hydantoin lesions. These studies also reveal that both NEIL1 and the UvrABC nuclease system use similar strategies that rely heavily on the local duplex stability to recognize a wide variety of structurally diverse lesions within DNA. During periods of high oxidative stress and oxidative DNA damage, the action of both BER and NER pathways would accelerate repair. Overlapping lesion specificity among DNA repair pathways would also be an evolutionary advantage, particularly for the highly mutagenic lesions Gh and Sp.[31]

■ ASSOCIATED CONTENT

Ⓢ Supporting Information

Kinetic data tables for edited and nonedited NEIL1 (Tables 1 and 2), EMSA experiments with UvrA (Figure 2), representative PAGE autoradiograms for UvrABC excision sites (Figure 1), representative kinetic plots for Sp−amine adduct removal by Fpg and NEIL1 (Figures 3 and 4), representative PAGE autoradiograms of footprinting with E3Q NEIL1 (Figure 5) and the corresponding histogram (Figure 6), and supplemen-

tary methods. This material is available free of charge via the Internet at http://pubs.acs.org.

AUTHOR INFORMATION

Corresponding Author

ssdavid@ucdavis.edu

Notes

The authors declare no competing financial interest.

ACKNOWLEDGMENTS

We thank the National Institutes of Health (Grant R01CA090689 to S.S.D. and C.J.B. and Grant 1R01ES019566 to B.V.H.) for support of this work. We also thank Professors Susan Wallace and Sylvie Doublie (University of Vermont, Burlington, VT) for the NEIL1 and Nei expression plasmids and Ms. Amelia Manlove for help in preparing figures and editing the manuscript. We also thank Dr. Sucharita Kundu for performing initial experiments that showed that Sp−amine adducts are substrates for NEIL1.

REFERENCES

(1) David, S. S.; O'Shea, V. L.; Kundu, S. *Nature* **2007**, *447*, 941.
(2) Neeley, W. L.; Essigmann, J. M. *Chem. Res. Toxicol.* **2006**, *19*, 491.
(3) Mangerich, A.; Knutson, C. G.; Parry, N. M.; Muthupalani, S.; Ye, W.; Prestwich, E.; Cui, L.; McFaline, J. L.; Mobley, M.; Ge, Z.; Taghizadeh, K.; Wishnok, J. S.; Wogan, G. N.; Fox, J. G.; Tannenbaum, S. R.; Dedon, P. C. *Proc. Natl. Acad. Sci. U.S.A.* **2012**, *109*, E1820.
(4) Burrows, C. J.; Muller, J. G.; Kornyushyna, O.; Luo, W.; Duarte, V.; Leipold, M. D.; David, S. S. *Environ. Health Perspect.* **2002**, *110* (Suppl. 5), 713.
(5) Luo, W.; Muller, J. G.; Rachlin, E. M.; Burrows, C. J. *Org. Lett.* **2000**, *2*, 613.
(6) Munk, B. H.; Burrows, C. J.; Schlegel, H. B. *J. Am. Chem. Soc.* **2008**, *130*, 5245.
(7) Fleming, A. M.; Burrows, C. J. *Chem. Res. Toxicol.* **2013**, *26*, 593.
(8) Fleming, A. M.; Muller, J. G.; Dlouhy, A. C.; Burrows, C. J. *J. Am. Chem. Soc.* **2012**, *134*, 15091.
(9) Luo, W.; Muller, J. G.; Rachlin, E. M.; Burrows, C. J. *Chem. Res. Toxicol.* **2001**, *14*, 927.
(10) Suzuki, T.; Masuda, M.; Friesen, M. D.; Ohshima, H. *Chem. Res. Toxicol.* **2001**, *14*, 1163.
(11) Suzuki, T.; Ohshima, H. *FEBS Lett.* **2002**, *516*, 67.
(12) Suzuki, T.; Friesen, M. D.; Ohshima, H. *Chem. Res. Toxicol.* **2003**, *16*, 382.
(13) Adam, W.; Arnold, M. A.; Grune, M.; Nau, W. M.; Pischel, U.; Saha-Moller, C. R. *Org. Lett.* **2002**, *4*, 537.
(14) Crean, C.; Geacintov, N. E.; Shafirovich, V. *Angew. Chem., Int. Ed.* **2005**, *44*, 5057.
(15) Crean, C.; Lee, Y. A.; Yun, B. H.; Geacintov, N. E.; Shafirovich, V. *ChemBioChem* **2008**, *9*, 1985.
(16) Joffe, A.; Geacintov, N. E.; Shafirovich, V. *Chem. Res. Toxicol.* **2003**, *16*, 1528.
(17) Niles, J. C.; Wishnok, J. S.; Tannenbaum, S. R. *Org. Lett.* **2001**, *3*, 963.
(18) Suzuki, T.; Masuda, M.; Friesen, M. D.; Fenet, B.; Ohshima, H. *Nucleic Acids Res.* **2002**, *30*, 2555.
(19) Yu, H.; Venkatarangan, L.; Wishnok, J. S.; Tannenbaum, S. R. *Chem. Res. Toxicol.* **2005**, *18*, 1849.
(20) Niles, J. C.; Wishnok, J. S.; Tannebaum, S. R. *Chem. Res. Toxicol.* **2004**, *17*, 1510.
(21) Johansen, M. E.; Muller, J. G.; Xu, X.; Burrows, C. J. *Biochemistry* **2005**, *44*, 5660.
(22) Xu, X.; Muller, J. G.; Ye, Y.; Burrows, C. J. *J. Am. Chem. Soc.* **2008**, *130*, 703.
(23) Hosford, M. E.; Muller, J. G.; Burrows, C. J. *J. Am. Chem. Soc.* **2004**, *126*, 9540.
(24) Hickerson, R. P.; Chepanoske, C. L.; Williams, S. D.; David, S. S.; Burrows, C. J. *J. Am. Chem. Soc.* **1999**, *121*, 9901.
(25) Schibel, A. E.; An, N.; Jin, Q.; Fleming, A. M.; Burrows, C. J.; White, H. S. *J. Am. Chem. Soc.* **2010**, *132*, 17992.
(26) Solivio, M. J.; Nemera, D. B.; Sallans, L.; Merino, E. J. *Chem. Res. Toxicol.* **2012**, *25*, 326.
(27) Kornyushyna, O.; Burrows, C. J. *Biochemistry* **2003**, *42*, 13008.
(28) Aller, P.; Ye, Y.; Wallace, S. S.; Burrows, C. J.; Doublie, S. *Biochemistry* **2010**, *49*, 2502.
(29) Kornyushyna, O.; Berges, A. M.; Muller, J. G.; Burrows, C. J. *Biochemistry* **2002**, *41*, 15304.
(30) Duarte, V.; Muller, J. G.; Burrows, C. J. *Nucleic Acids Res.* **1999**, *27*, 496.
(31) Henderson, P. T.; Delaney, J. C.; Muller, J. G.; Neeley, W. L.; Tannenbaum, S. R.; Burrows, C. J.; Essigmann, J. M. *Biochemistry* **2003**, *42*, 9257.
(32) Leipold, M. D.; Muller, J. G.; Burrows, C. J.; David, S. S. *Biochemistry* **2000**, *39*, 14984.
(33) Leipold, M. D.; Workman, H.; Muller, J. G.; Burrows, C. J.; David, S. S. *Biochemistry* **2003**, *42*, 11373.
(34) Hailer, M. K.; Slade, P. G.; Martin, B. D.; Rosenquist, T. A.; Sugden, K. D. *DNA Repair* **2005**, *4*, 41.
(35) Krishnamurthy, N.; Muller, J. G.; Burrows, C. J.; David, S. S. *Biochemistry* **2007**, *46*, 9355.
(36) Krishnamurthy, N.; Zhao, X.; Burrows, C. J.; David, S. S. *Biochemistry* **2008**, *47*, 7137.
(37) Hazra, T. K.; Muller, J. G.; Manuel, R. C.; Burrows, C. J.; Lloyd, R. S.; Mitra, S. *Nucleic Acids Res.* **2001**, *29*, 1967.
(38) Tretyakova, N. Y.; Wishnok, J. S.; Tannenbaum, S. R. *Chem. Res. Toxicol.* **2000**, *13*, 658.
(39) Liu, M.; Bandaru, V.; Holmes, A.; Averill, A. M.; Cannan, W.; Wallace, S. S. *Protein Expression Purif.* **2012**, *84*, 130.
(40) Bandaru, V.; Zhao, X.; Newton, M. R.; Burrows, C. J.; Wallace, S. S. *DNA Repair* **2007**, *6*, 1629.
(41) Yeo, J.; Goodman, R. A.; Schirle, N. T.; David, S. S.; Beal, P. A. *Proc. Natl. Acad. Sci. U.S.A.* **2010**, *107*, 20715.
(42) Zhao, X.; Krishnamurthy, N.; Burrows, C. J.; David, S. S. *Biochemistry* **2010**, *49*, 1658.
(43) Hailer, M. K.; Slade, P. G.; Martin, B. D.; Sugden, K. D. *Chem. Res. Toxicol.* **2005**, *18*, 1378.
(44) Chan, M. K.; Ocampo-Hafalla, M. T.; Vartanian, V.; Jaruga, P.; Kirkali, G.; Koenig, K. L.; Brown, S.; Lloyd, R. S.; Dizdaroglu, M.; Teebor, G. W. *DNA Repair* **2009**, *8*, 786.
(45) Truglio, J. J.; Croteau, D. L.; Van Houten, B.; Kisker, C. *Chem. Rev.* **2006**, *106*, 233.
(46) Minko, I. G.; Zou, Y.; Lloyd, R. S. *Proc. Natl. Acad. Sci. U.S.A.* **2002**, *99*, 1905.
(47) Van Houten, B. *Microbiol. Rev.* **1990**, *54*, 18.
(48) Van Houten, B.; McCullough, A. *Ann. N.Y. Acad. Sci.* **1994**, *726*, 236.
(49) Wang, H.; DellaVecchia, M. J.; Skorvaga, M.; Croteau, D. L.; Erie, D. A.; Van Houten, B. *J. Biol. Chem.* **2006**, *281*, 15227.
(50) Croteau, D. L.; DellaVecchia, M. J.; Wang, H.; Bienstock, R. J.; Melton, M. A.; Van Houten, B. *J. Biol. Chem.* **2006**, *281*, 26370.
(51) Imoto, S.; Bransfield, L. A.; Croteau, D. L.; Van Houten, B.; Greenberg, M. M. *Biochemistry* **2008**, *47*, 4306.
(52) Zhao, X.; Muller, J. G.; Halasyam, M.; David, S. S.; Burrows, C. J. *Biochemistry* **2007**, *46*, 3734.
(53) Skorvaga, M.; Theis, K.; Mandavilli, B. S.; Kisker, C.; Van Houten, B. *J. Biol. Chem.* **2002**, *277*, 1553.
(54) McKibbin, P. L.; Kobori, A.; Taniguchi, Y.; Kool, E. T.; David, S. S. *J. Am. Chem. Soc.* **2012**, *134*, 1653.
(55) Minko, I. G.; Kurtz, A. J.; Croteau, D. L.; Van Houten, B.; Harris, T. M.; Lloyd, R. S. *Biochemistry* **2005**, *44*, 3000.
(56) Sambrook, J.; Russell, D. W. *Molecular Cloning, A Laboratory Manual*, 3rd ed.; Cold Spring Harbor Laboratory Press: Plainview, NY, 2001; Vol. *1*.

(57) Zou, Y.; Van Houten, B. *EMBO J.* **1999**, *18*, 4889.
(58) Zou, Y.; Luo, C.; Geacintov, N. E. *Biochemistry* **2001**, *40*, 2923.
(59) Webster, M. P. J.; Jukes, R.; Zamfir, V. S.; Kay, C. W. M.; Bagnéris, C.; Barrett, T. *Nucleic Acids Res.* **2012**, *40*, 8743.
(60) Pakotiprapha, D.; Samuels, M.; Shen, K.; Hu, J. H.; Jeruzalmi, D. *Nat. Struct. Mol. Biol.* **2012**, *19*, 291.
(61) Chu, A. M.; Fettinger, J. C.; David, S. S. *Bioorg. Med. Chem. Lett.* **2011**, *21*, 4969.
(62) Liu, Y.; Reeves, D.; Kropachev, K.; Cai, Y.; Ding, S.; Kolbanovskiy, M.; Kolbanovskiy, A.; Bolton, J. L.; Broyde, S.; Van Houten, B.; Geacintov, N. E. *DNA Repair* **2011**, *10*, 684.
(63) Truglio, J. J.; Karakas, E.; Rhau, B.; Wang, H.; DellaVecchia, M. J.; Van Houten, B.; Kisker, C. *Nat. Struct. Mol. Biol.* **2006**, *13*, 360.
(64) Hughes, C.; Wang, H.; Ghodke, H.; Simons, M.; Towheed, A.; Peng, Y.; Van Houten, B.; Kad, N. *Nucleic Acids Res.* **2013**, *41*, 4901.
(65) Malta, E.; Verhagen, C. P.; Mollenaar, G. F.; Fillipov, D. V.; van der Marel, G. A.; Goosen, N. *DNA Repair* **2008**, *7*, 1647.
(66) Malta, E.; Moolenar, G. F.; Goosen, N. *J. Biol. Chem.* **2006**, *281*, 2184.
(67) Jia, L.; Shafirovich, V.; Shapiro, R.; Geacintov, N. E.; Broyde, S. *Biochemistry* **2005**, *44*, 13342.
(68) Yennie, C. J.; Delaney, S. *Chem. Res. Toxicol.* **2012**, *25*, 1732.
(69) Jia, L.; Shafirovich, V.; Shapiro, R.; Geacintov, N. E.; Broyde, S. *Biochemistry* **2005**, *44*, 6043.
(70) Prakash, A.; Doublie, S.; Wallace, S. S. *Prog. Mol. Biol. Transl. Sci.* **2012**, *110*, 71.
(71) Hazra, T. K.; Izumi, T.; Boldogh, I.; Imhoff, B.; Kow, Y. W.; Jaruga, P.; Dizdaroglu, M.; Mitra, S. *Proc. Natl. Acad. Sci. U.S.A.* **2002**, *99*, 3523.
(72) Hu, J.; de Souza-Pinto, N. C.; Haraguchi, K.; Hogue, B. A.; Jaruga, P.; Greenberg, M. M.; Dizdaroglu, M.; Bohr, V. A. *J. Biol. Chem.* **2005**, *280*, 40544.
(73) Jaruga, P.; Birincioglu, M.; Rosequist, T. A.; Dizdaroglu, M. *Biochemistry* **2004**, *43*, 15909.
(74) Roy, L. M.; Jaruga, P.; Wood, T. G.; McCullough, A. K.; Dizdaroglu, M.; Lloyd, R. S. *J. Biol. Chem.* **2007**, *282*, 15790.
(75) Hazra, T. K.; Kow, Y. W.; Hatahet, Z.; Imhoff, B.; Boldogh, I.; Mokkapanti, S. K.; Mitra, S.; Izumi, T. *J. Biol. Chem.* **2002**, *277*, 30417.
(76) Bandaru, V.; Sunkara, S.; Wallace, S. S.; Bond, J. P. *DNA Repair* **2002**, *1*, 517.
(77) Takao, M.; Kanno, S.; Kobayashi, K.; Zhang, Q.-M.; Yonei, S.; van der Horst, G. T. J.; Yasui, A. *Proc. Natl. Acad. Sci. U.S.A.* **2002**, *277*, 42205.
(78) Couve, S.; Mace-Aime, G.; Rosselli, F.; Saparbaev, M. *J. Biol. Chem.* **2009**, *284*, 11963.
(79) Couve-Privat, S.; Mace-Aime, G.; Rosselli, F.; Saparbaev, M. *Nucleic Acids Res.* **2007**, *35*, 5672.
(80) Chinyengetere, F.; Jamieson, E. R. *Biochemistry* **2008**, *47*, 2584.
(81) Imamura, K.; Averill, A.; Wallace, S. S.; Doublie, S. *J. Biol. Chem.* **2012**, *287*, 4288.
(82) Desai, S. D.; Zhang, H.; Rodriguez-Bauman, A.; Yang, J. M.; Wu, X.; Gounder, M. K.; Rubin, E. H.; Liu, L. F. *Mol. Cell. Biol.* **2003**, *23*, 2341.
(83) Mao, Y.; Desai, S. D.; Ting, C. Y.; Hwang, J.; Liu, L. F. *J. Biol. Chem.* **2001**, *276*, 40652.
(84) Quievryn, G.; Zhitkovich, A. *Carcinogenesis* **2000**, *21*, 1573.
(85) Baker, D. J.; Wuenschell, G.; Xia, L.; Termini, J.; Bates, S. E.; Riggs, A. D.; O'Connor, T. R. *J. Biol. Chem.* **2007**, *282*, 22592.
(86) Jaruga, P.; Xiao, Y.; Vartanian, V.; Lloyd, R. S.; Dizdaroglu, M. *Biochemistry* **2010**, *49*, 1053.
(87) Muftuoglu, M.; de Souza-Pinto, N. C.; Dogan, A.; Aamann, M.; Stevnsner, T.; Rybanska, I.; Kirkali, G.; Dizdaroglu, M.; Bohr, V. A. *J. Biol. Chem.* **2009**, *284*, 9270.
(88) Tuo, J.; Jaruga, P.; Rodriguez, H.; Dizdaroglu, M.; Bohr, V. A. *J. Biol. Chem.* **2002**, *277*, 30832.
(89) Sunesen, M.; Stevnsner, T.; Brosh, R. M., Jr.; Dianov, G. L.; Bohr, V. A. *Oncogene* **2002**, *21*, 3571.
(90) Stevnsner, T.; Nyaga, S.; de Souza-Pinto, N. C.; van der Horst, G. T.; Gorgels, T. G.; Hogue, B. A.; Thorslund, T.; Bohr, V. A. *Oncogene* **2002**, *21*, 8675.
(91) Kyng, K. J.; May, A.; Brosh, R. M., Jr.; Cheng, W. H.; Chen, C.; Becker, K. G.; Bohr, V. A. *Oncogene* **2003**, *22*, 1135.
(92) Hanawalt, P. C. *Science* **1994**, *266*, 1957.
(93) Hanawalt, P. C. *Nature* **2000**, *405*, 415.
(94) Friedberg, E. C.; Henning, K. A. *Mutat. Res.* **1993**, *289*, 47.